Single-neuron representations of spatial memory targets in humans

Melina Tsitsiklis[1], Jonathan Miller[2], Salman E. Qasim[2], Cory S. Inman[3], Robert E. Gross[3], Jon T. Willie[3], Elliot H. Smith[4], Sameer A. Sheth[5], Catherine A. Schevon[6], Michael R. Sperling[7], Ashwini Sharan[8], Joel M. Stein[9], Joshua Jacobs[*2]

[1]Doctoral Program in Neurobiology and Behavior, Columbia University, NY, NY 10027, USA
[2]Department of Biomedical Engineering, Columbia University, NY, NY 10027, USA
[3]Emory University School of Medicine, Atlanta, GA 30322, USA
[4]Department of Neurosurgery, University of Utah, Salt Lake City, UT 84112, USA
[5]Department of Neurosurgery, Baylor College of Medicine, Houston, TX 77030, USA
[6]Department of Neurology, Columbia University Medical Center, NY, NY 10032, USA
[7]Department of Neurology, Thomas Jefferson University, Philadelphia, PA 19107, USA
[8]Department of Neurosurgery, Thomas Jefferson University, Philadelphia, PA 19107, USA
[9]Department of Radiology, Hospital of the University of Pennsylvania, Philadelphia, PA 19104, USA

[*]Correspondence: joshua.jacobs@columbia.edu, 351 Engineering Terrace, Mail Code 8904, 1210 Amsterdam Avenue, New York, NY 10027, 212-854-2445

Summary

The hippocampus and surrounding medial-temporal-lobe (MTL) structures are critical for both memory and spatial navigation (Scoville and Milner, 1957; Morris et al., 1982). Much research has focused on neurons that activate according to an animal's own spatial properties, such as "place cells" that represent the current location (O'Keefe and Dostrovsky, 1971), or "head-direction cells" that code for the current heading (Taube et al., 1990). In addition to representing the current spatial setting, these same MTL structures are important for other behaviors such as memory, which can involve remote locations among other contextual information (Schiller et al., 2015; Epstein et al., 2017). However, the human cellular representations that underlie our ability to form memories that involve remote locations are unclear. We recorded single-neuron activity from neurosurgical patients playing Treasure Hunt (TH), a virtual-reality object–location memory task. We found that the activity of many MTL neurons was significantly modulated by the position of the to-be-remembered object. In addition, we observed neurons whose firing rates during navigation were explained by the subject's heading direction, and others that predicted subsequent memory performance. By showing evidence for neurons encoding remote locations that are the targets of memory encoding, our results suggest that the human MTL represents to-be-remembered locations in service of memory formation.

Results

Humans have rich navigation and spatial memory skills, including the ability to not only accurately navigate through complex environments but also to imagine and remember events that occur at remote locations (Spiers and Maguire, 2007; Miller et al., 2013; Ekstrom, 2015; Vass et al., 2016). We hypothesized that the types of neural activity in the human MTL that represent one's current location during navigation are also involved in representing relevant remote locations during spatial cognition. To examine this issue directly, we asked neurosurgical patients with microelectrodes implanted in their MTL to play a virtual-reality spatial-memory task, and we examined how their neural responses related to their simultaneous movement and memory. The fifteen participants in our study played Treasure Hunt (TH), a video-game–like task that measures subjects' ability to remember the spatial locations where various objects are hidden (Miller et al., 2018). In each trial of the task, subjects explored a virtual beach and traveled to a series of treasure chests. Upon reaching each chest, it opened and an object appeared. The subject's goal was to encode the spatial location corresponding to the position

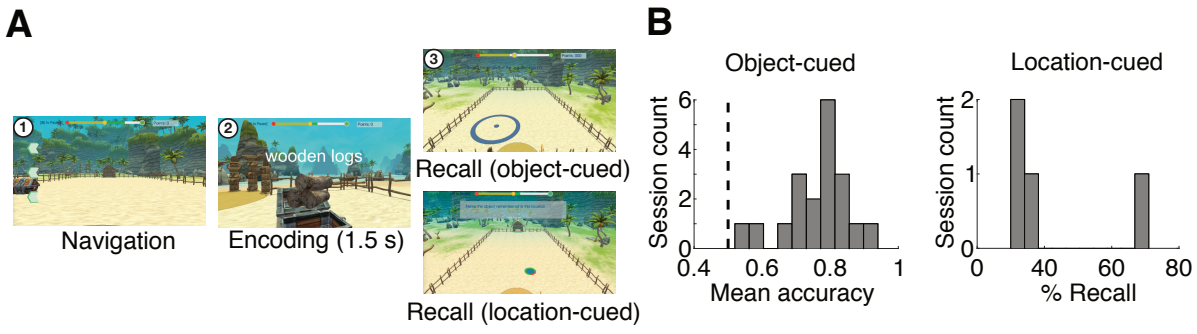

Figure 1: Treasure Hunt (TH) task performance. *A. Screen images from the Navigation, Encoding, and Recall phases of TH. The two images for the recall phase correspond to different versions of the task (see Methods). B. Histogram showing mean performance on the recall phase of TH in each of the two task versions.*

of each item. To characterize the neural basis of spatial memory, we analyzed the neural recordings to identify neurons that represented memory target locations, as well as the subject's current virtual location, heading direction, and subsequent memory performance.

Behavior. Before characterizing neural signatures of spatial memory encoding, we first examined subjects' behavior in TH (Figure 1a). In each trial subjects navigated to chests ("Navigation"), and upon reaching each chest viewed an object whose location they tried to encode ("Encoding"). Finally, in the "Recall" phase subjects were asked to recall the object locations. The subjects in our study performed one of two task versions, which differed in terms of the Recall phase. In the "object-cued" version, they viewed the image of a cued object and indicated its location by moving an on-screen cursor accordingly. In the "location-cued" version of the task they viewed a probed location and verbally responded by speaking the name of the corresponding object into a microphone.

We scored behavioral performance during the recall phase as a measure of subjects' object–location memory. Subjects showed good performance in both versions of the task (Figure 1b), indicating that they were successfully able to orient and remember locations in our virtual reality environment. Mean accuracy on all object-cued sessions was above chance (chance=0.5). The mean performance on location-cued sessions (43%) was consistent with levels seen in other paired-associate memory tasks that required verbal responses, such as in Greenberg et al. (2015) where subjects exhibited 40% recall rates.

Neurons responsive to the current memory target. We hypothesized that we would observe "memory target cells," which we defined as neurons whose activity was modulated by the location of the current, to-be-remembered chest as subjects drove to it during navigation. We were motivated by previous work in animal models showing MTL cells that represent salient remote locations (Rolls and O'Mara, 1995; Wilming et al., 2018; Wirth et al., 2017; Omer et al., 2018; Danjo et al., 2018; Gauthier and Tank, 2018), as well as related evidence from recordings of human theta oscillations (Lee et al., 2018) and fMRI (Brown et al., 2016). Therefore, we examined how neuronal firing rates during navigation varied according to the location of the current target chest. We identified single-neuron action potentials (Fried et al., 1999), and isolated a total of 131 putative MTL neurons across 23 task sessions. Forty-five of these neurons were in the hippocampal formation (HF) and 86 were in the parahippocampal gyrus (PHG).

To identify these "memory target cells," we analyzed each cell's spiking activity as a function of the location of the upcoming chest, in addition to the subject's current position (Fig. 2a). We generated firing rate heatmaps both based on the location of the upcoming memory target, as well as the subject's own position. We identified neurons whose firing rates were significantly modulated using permutation tests.

We labeled neurons as memory-target cells if their firing rate significantly varied as function of the chest location. Figure 2b illustrates the activity of one example memory-target cell from the left entorhinal cortex (EC) of Patient 9. This neuron increased its firing rate when the subject navigated to chests that were located in the "south-central" part of the environment ($p < 0.001$). Critically, while this cell's firing rate was modulated by the location of the upcoming object, it did not vary significantly according to the subject's own position (Figure 2b-right, $p = 0.437$). Thus, this neuron's representation of the current navigational target constitutes a novel coding pattern that is distinct from the activity of conventional place cells, which generally represent an animal's own location. Figure 2c shows a second example of this phenomenon from a cell in Patient 12's right EC, which significantly increased its firing rate when the subject had memory targets in the "east" section of the

environment ($p = 0.004$), and did not show a firing-rate modulation according to the subject's own position ($p = 0.49$).

Across the population, 20% of MTL cells (26 of 131) had firing rates that were significantly modulated by memory target location, which is significantly greater than the 5% expected by chance ($p < 0.01$, binomial test). The number of these memory-target cells that we observed was significantly above chance both when measured separately for the HF and for the PHG regions (binomial tests p's< 0.01). None of these cells' firing rates were modulated by the subject's virtual position. Thus, these results indicate that a substantial number of neurons throughout the human MTL specifically represent remote locations in a task when they are important behaviorally.

Given the large literature on place cells (Muller, 1996), we also characterized neurons whose firing rates were modulated by the subject's current position. Figure 3 shows three example cells that showed significant spatial modulation according to the subject's current virtual location. We found that during navigation some cells individually exhibited significant place coding, but at the population level the total number of observed place-like cells was not above chance. Across the population 8 of 131 (6%) of MTL cells were significantly modulated by subject position (Fig. 3d) ($p = 0.21$, binomial test).

Neurons responsive to heading direction. In rodents there is evidence for neurons whose firing rates are modulated by the direction of the animal's head during movement (Taube et al., 1990; Robertson et al., 1999). These head-direction cells were first discovered in the dorsal presubiculum and are also commonly found in the anterodorsal thalamus, but have also been found in areas of the MTL such as the entorhinal cortex (Sargolini et al., 2006). These cells have not previously been found in humans, but the representation of heading direction could play a role in forming memories. As such, we tested for the existence of "heading-direction" cells in our dataset, which we defined as neurons that varied their firing rate according to the direction that subjects moved in the virtual environment, grouped into four 90° bins, which we refer to as north, south, east, and west. Figure 4a–d illustrates the activity of four significant heading-direction cells. As these examples illustrate, the heading that elicited peak firing activity varied across individual heading-direction cells. In addition, some cells showed increased firing rates at multiple distinct headings (Figure 4c–d), similar to "bidirectional cells" recently observed in rodents (Jacob et al., 2017). We did not find that any particular preferred angle was dominant across the population of heading-direction cells (Figure 4e).

Overall, 12% of MTL cells (16 of 131) were heading-direction cells, showing significant changes in firing rate according to the virtual heading, which is more than expected by chance ($p < 0.0003$, binomial test). There were significant proportions of heading-direction cells in both the HF and PHG ($p = 0.007$ and $p = 0.004$, respectively; Figure 2f). No heading-direction cells showed firing rates that varied with the subject's current position; two heading-direction cells showed effects of memory target position. Because the population of cells modulated by heading direction is largely nonoverlapping from those that were significantly modulated by memory target position, it suggests that our finding of memory-target cells is not explained by direction-related modulations.

Neurons modulated by subsequent memory performance. We next tested whether each cell's firing rate during navigation significantly varied as a function of whether or not memory targets were subsequently remembered (Miller et al., 2018). Figure 5a–b shows two example "memory cells" whose firing rates during navigation significantly varied according to whether or not the subject subsequently recalled the correct location of the item in the current chest. As illustrated by these examples, individual cells showed either significant increases or decreases in their firing rate according to subsequent memory performance.

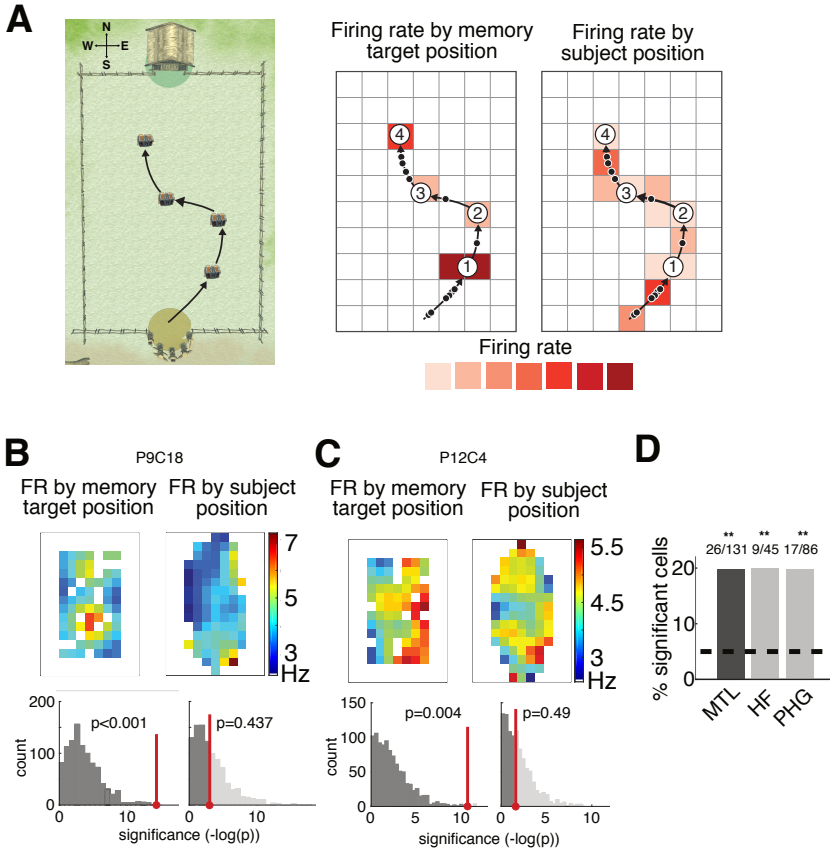

Figure 2: Neural activity related to memory target position. *A. Analysis framework for binning navigation period neuronal data by subject position and memory target location, shown for an example trial. Left, overhead view of TH environment with example paths to 4 chests (only one chest is visible at a given time). Middle, example path spikes binned by memory target location to calculate firing rate during navigation based on the chest location. Right, same spikes binned by subject position to calculate firing rate on the path. B. Top-left, firing rate map of navigation activity binned by memory target position for a neuron in the left EC from Patient 9. Black line indicates the perimeter of the traversable virtual environment. Bottom-left, histogram of p-values from ANOVA (see Methods) assessing memory target location modulation of firing rate for the observed data (red) versus shuffled data (gray). This cell's activity is significantly modulated by the memory target position (permutation-corrected ANOVA, $p < 0.001$). Top-right, firing rate map for current location. Bottom-right, histogram of p-values from ANOVA assessing current location modulation of firing rate . Neuron is not significantly modulated by subject position ($p = 0.437$). C. Same as B but for another example neuron in the right EC from Patient 12. Neuron is significantly modulated by memory target position ($p = 0.004$) and not subject position ($p = 0.49$). D. Percentage of significant memory-target cells by region. Shown for all MTL neurons and also split into HF and PHG. ** indicates $p < 0.01$ for binomial test.*

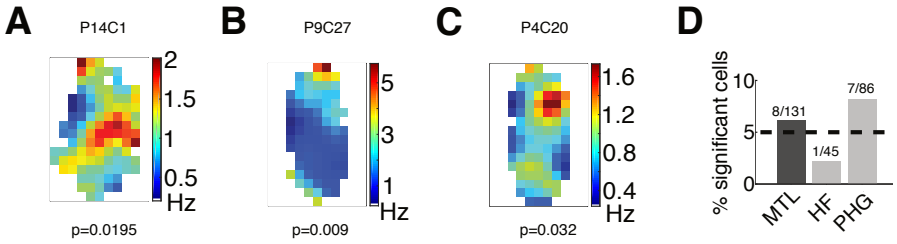

Figure 3: Neural activity related to the subject's current location. *A. Firing rate map of navigation activity binned by subject location for a right parahippocampal cortex neuron from Patient 14. This cell's activity is significantly modulated by the subject's virtual position (permutation-corrected ANOVA, $p = 0.0195$). B. Example cell from left EC in Patient 9 ($p = 0.009$). C. Example neuron from Patient 4 in right EC. Neuron is significantly modulated by subject position ($p = 0.032$). D) Percentage of significant spatially-tuned cells by region. ** indicates $p < 0.01$ for binomial test.*

Twelve MTL neurons (9%) showed significant changes in firing rate in relation to subsequent memory performance, which is greater than the 5% expected by chance ($p = 0.014$, binomial test). This effect was most prominent in the PHG ($p = 0.011$, binomial test; Fig. 5d). Of the twelve cells that showed significant memory-related firing-rate changes, seven demonstrated significant memory-related firing rate increases while five showed significant decreases (see Figure 5C). Of the 12 memory cells, zero were place-like cells, 3 were memory-target cells, and 2 were heading-direction cells.

Discussion

In this study, we found that the firing rates of subjects' MTL cells were modulated by the locations of to-be-remembered targets, heading direction, and subsequent memory performance, but not by self location. By showing that single-neuron activity in the human MTL can represent remote spatial information, these results help explain how contextual information, such as relevant remote locations, may be used to support memory formation in humans.

Several other studies have described MTL activity in animals with spatial responses that are related to our findings in humans. The existence of hippocampal "spatial view" cells in non-human primates provides one possible explanation for the memory-target cells we describe (Rolls and O'Mara, 1995; Wirth et al., 2017). Those studies characterized how MTL neurons code for remote spatial locations, and our study extends this area of research to relate to memory encoding. Furthermore, there is recent evidence of entorhinal grid cells coding for viewed locations in 2D (Wilming et al., 2018), as well as view-related sharp-wave-ripple responses in the primate hippocampus (Leonard and Hoffman, 2017). Additionally, "social place cells," whose activity reflect allocentric representations of conspecifics, are another example of coding for salient locations albeit not for memory targets (Omer et al., 2018; Danjo et al., 2018). Finally, the cells we describe may be related to the view cells found by Ekstrom et al. (2003). However, whereas Ekstrom et al.'s view cells represent visually distinctive buildings, the memory-target cells we describe represent locations that are denoted by identical treasure chests. Thus, our study adds to the growing evidence that MTL neurons can be modulated as a function of salient remote spatial locations.

In addition to our primary finding of neurons that activate for remote target locations, we also observed other types of navigationally relevant neural responses. The first of these are heading-direction cells, in which we provide some of the first evidence of this cell type in humans. Head-

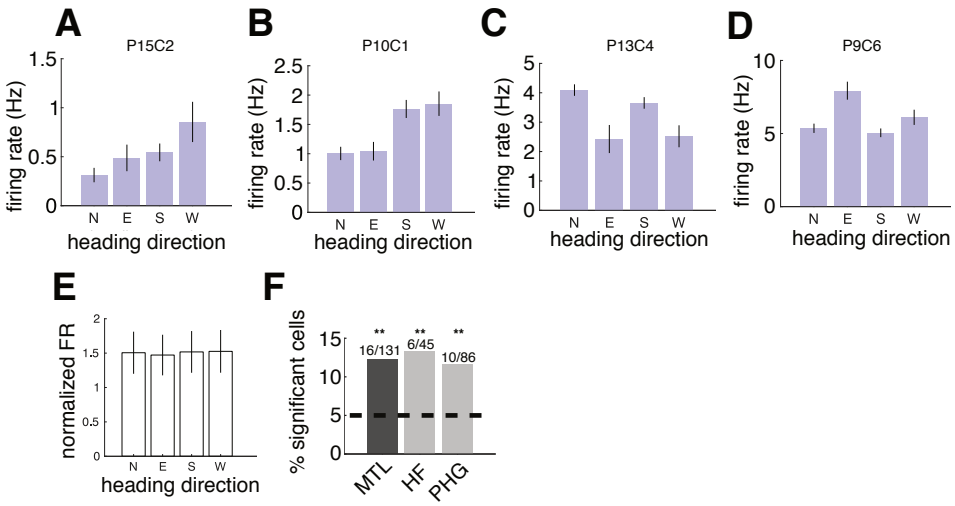

Figure 4: Neural activity related to the subject's heading. *Firing rate by heading direction (split by N=north, E=east, S=south, W=west) for example cells significantly modulated by heading direction. Error bars are SEM of each group. A) Example cell from Patient 15, in the left hippocampus, significantly modulated by heading direction ($p = 0.026$). B. Example cell from Patient 10, in the left parahippocampal cortex, significantly modulated by heading direction ($p = 0.005$). C-D. Two more significant heading-direction cells in the left hippocampus and left EC respectively (from Patient 13; $p = 0.0315$, from Patient 9; $p = 0.0015$). E. Average of z-scored firing rates for each cell split by heading direction, across all significant heading-direction cells. F. Percentage of significant heading-direction cells by region. ** indicates $p < 0.01$ for binomial test.*

direction cells have been described extensively in rodents and are most frequently found in areas such as the postsubiculum, retrosplenial cortex, anterodorsal thalamus (Taube et al., 1990; Taube, 1998; Robertson et al., 1999). However, they have also been found in the hippocampus and entorhinal cortex (Leutgeb et al., 2000; Sargolini et al., 2006). In addition to the cells we found that respond most to movement in a single direction, we also found evidence of cells with bidirectional responses, which are similar to patterns reported recently in rodents (Jacob et al., 2017).

Finally, we observed neurons that varied their firing rates during navigation according to subsequent memory performance. Human fMRI studies consistently report greater hippocampal BOLD activity for subsequent memory (Schacter and Wagner, 1999; Chua et al., 2007; Suthana et al., 2009). However, few studies have found that single-neuron firing rates relate to episodic memory in the human hippocampus and surrounding MTL. For example, Rutishauser et al. (2010) found that mean firing rates during learning did not differ as a function of subsequent memory performance. Here we found cells whose firing rates significantly increased for successful memory encoding and others whose firing significantly decreased. This variability could explain why previous studies of population neural signals did not find a consistent firing-rate response relating to subsequent memory, because the mixed patterns from individual neurons may cancel at the population level. In accordance with our results, Wixted et al. (2014) report evidence of a sparse and distributed code of episodic memory in human hippocampus, which is consistent with our finding that individual neurons showed both increases and decreases in firing rates during successful memory encoding.

In light of the literature on place cells in rodents (O'Keefe and Dostrovsky, 1971), monkeys (Wirth et al., 2017; Gulli et al., 2018), and humans (Ekstrom et al., 2003), it might be considered surprising that we did not observe a large proportion of neurons with activity that varied as a function of the subject's own location. As we describe below, this pattern may have stemmed from the behavioral demands of our task, which differed compared to the paradigms used previously to study human

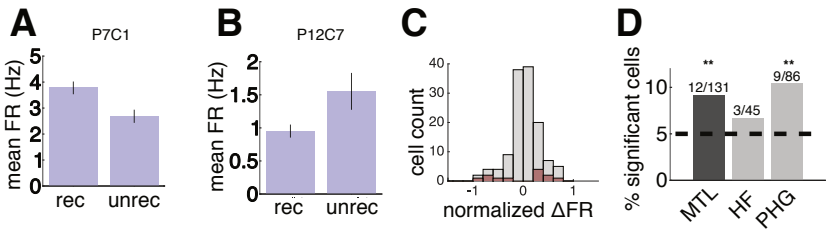

Figure 5: Neural activity related to subsequent memory. *Firing rate by subsequent memory performance for two example cells significantly modulated by subsequent recall. Error bars are SEM of the trial means in each condition. A. Example neuron from Patient 7 in the left PRC, significantly modulated by subsequent memory ($p = 0.017$). B. Example neuron from Patient 12 in the right EC, $p = 0.044$. C. Histogram of cell count by normalized firing rate between conditions ((rec-unrec)/rec). Red indicates the significant cells. D. Percentage of significant memory-related cells by region. ** indicates $p < 0.01$ for binomial test.*

single-neuron electrophysiology in navigation. We hypothesize that the nature of the MTL's spatial coding varies with task demands. In our experiment, on each trial subjects remembered the positions of objects that had been placed at locations in an open environment that were subsequently unmarked. Therefore, this task allowed us to examine neural activity used to represent new spatial locations for memory formation. On each trial in our task, new, previously unmarked locations become salient and relevant for memory encoding. This may have led to greater attentional focus to those upcoming locations during navigation instead of the subject's current location. However, in other tasks where the environmental structure was fairly static, subjects were likely to focus more on their current location, which would have been more likely to elicit place-cell activity (e.g. Ekstrom et al., 2003; Jacobs et al., 2010, 2013; Miller et al., 2013, 2015; Watrous et al., 2018; Qasim et al., 2018).

Our primary result is that single neurons in the human MTL code for remote locations that are relevant for memory. We also find coding of heading direction and subsequent memory. A remaining open question is whether the neuronal representation of memory targets relates specifically to where subjects are viewing, and future work utilizing eye tracking will be able to address this directly. By showing human MTL neuronal activity related to the location of upcoming memory targets rather than a subject's own location, our findings indicate that the human hippocampal system changes the nature of its representation to support task demands. This opens new directions for future research on what causes these representational schemes to change and how the brain links between different types of representations for individual memories.

Methods

Experimental Task

The subjects in our study were neurosurgical patients, who performed one of two versions of the Treasure Hunt (TH) task (referred to as 'object-cued' and 'location-cued' in Figure 1a). TH is a 3D virtual spatial-memory game developed in Unity3D. Subjects played TH on a bedside laptop computer and controlled their movement with a handheld joystick. In each trial of the task subjects explored a virtual beach (100×70 virtual units) to reach treasure chests that revealed hidden objects, with the goal of encoding the location of each encountered item. For a more detailed description of the object-cued task, see Miller et al. (2018). Briefly, the main components of the task are the Navigation, Encoding, and Retrieval phases. The focus of this paper is on the Navigation period.

Each trial of the object-cued task begins with navigation to a chest (i.e., the Navigation phase)

using a joystick. Upon arrival at the chest, the chest opens and either reveals an object or is empty. The subjects remain facing the open chest for 1.5 s (Encoding phase). In each trial the subjects navigate to a sequence of 4 chests. Two or three (randomly selected) of the chests contain an object and the rest are empty. In each session there are a total of 100 full chests and 60 empty chests, over 40 trials. In each trial the chests are placed in random locations such that their locations span the environment across trials, and they are never located in the outermost positions in the environment. After all four chests have been reached in each trial, subjects are transported automatically so they view the environment from an overhead perspective. They then perform a distractor minigame before entering the Recall phase. In Recall subjects are cued with each of the objects from the trial in a random sequence and asked to recall their location by placing the cursor in the correct location from the overhead view.

The location-cued task is a variation of the object-cued version with a different Recall phase, in which the subjects are cued with a location and asked to verbally recall the corresponding object. Each session of this task version consists of 30 trials, each with 3 or 4 chests, for a total of 105 chests per session. None of the chests are empty. During the Recall phase subjects are probed with 4 or 5 locations, one of which is a lure location that does not match the location of any of the trial's objects.

Intracranial Recordings

Fifteen patients (10 Male, mean age=32 years, minimum age=20 years) with medication-resistant epilepsy participated in this study. Subjects underwent a surgical procedure in which depth electrodes were implanted to localize epileptogenic regions at 3 different hospital sites (Columbia University Medical Center, Emory University School of Medicine, Thomas Jefferson University). Electrode placement was determined solely by the clinical team at each collaborating hospital. Behnke-Fried microelectrodes with 9 platinum–iridium microwires (40 μm) extending from the macroelectrode tip were implanted in the participating subjects following previously reported methods (Fried et al., 1999; Misra et al., 2014). All patients provided informed consent for both the Behnke-Fried implants and the behavioral task, under IRB protocols are all three institutions. The microwire data were recorded at 30 kHz using NeuroPort recording systems (Blackrock Microsystems, Salt Lake City, UT). We conducted automatic spike detection and sorting in Combinato (Niediek et al., 2016) and followed by manual sorting to identify putative single neurons following criteria described in Valdez et al. (2013).

Subjects participated in a total of 23 TH sessions. Across these sessions we successfully isolated a total of 131 putative neurons from microelectrodes localized to the medial temporal lobe (MTL). Forty-five of these neurons were in the HF: hippocampus and subiculum, and 86 were in the PHG: EC, perirhinal cortex, amygdala, and parahippocampal cortex (see Table 1) .

Behavioral performance

We assessed performance on the object-cued task as in earlier work (Miller et al., 2018). For each object the distance error is defined as the Euclidean distance between the subject's response and the correct location. Accuracy is defined as 1 minus the percentile rank of the actual distance error computed relative to the distribution of all possible distance errors that could have been made for the object's location. Performance on the location-cued task was calculated as the percentage of words correctly freely recalled.

Anatomical localization

We determined the anatomical location of each microwire electrode bundle by co-registering the pre-surgical T1 and T2 weighted structural MRIs to the post-surgical CT scan. Only subjects with depth electrodes extending into the MTL were included in this study. MTL subregions were automatically labeled using a multi-atlas based segmentation technique on the T2-weighted MRI. A neuroradiologist identified the electrode contacts on the post-surgical CT. Electrode contact coordinates were then mapped to MRI space and a neuroradiologist manually determined the anatomical locations of the microwire electrodes based on the co-registered images.

Analysis of spatial coding during navigation epochs

We analyzed neural data collected from the navigation periods of each task session. The rectangular environment was binned into a 5×7 grid, and both the current location and current memory target location were logged for each navigation epoch. For the data from a grid location to be used in the analysis, the subject must have occupied that location for a minimum of 5 s or 2 s when binning by subject position or memory target position, respectively. We discretized the behavioral navigation data into 100-ms epochs, and calculated the subject's current average x- and y-coordinate, current chest x- and y-coordinate, and speed within each 100-ms bin. We excluded navigation epochs during which subjects were not moving for more than 500 ms from the analyses. We binned the spike data into the corresponding 100-ms epochs and calculated the firing rate for each spatial bin. We calculated firing rate by subject position using the subject's virtual position, and firing rate by memory target position using each path's corresponding chest location.

We identified spatially modulated cells using an ANOVA to predict firing rate with current and memory target location as predictors. We assessed statistical significance using random circular permutation, as in earlier work (Ekstrom et al., 2003; Miller et al., 2015). This procedure was repeated 1000 times with circularly time-shifted firing rate values, whereby the firing rate of the cell was randomly shifted relative to the behavioral navigation data. If the test statistic calculated on the real data was in the 95^{th} percentile of the test statistics from the shifted data, the parameter was considered a significant factor in modulating firing rate.

To test for modulation of firing rate by heading direction, a separate ANOVA was conducted with heading quadrant (N,E,S,W) as a factor. The heading direction was determined using the x,y coordinates of the path and calculating the movement angle. To test for modulation of firing rate by subsequent memory another separate ANOVA was conducted with memory performance as a factor.

For each cell-type category, we tested the proportion of significant cells against the null hypothesis that the proportion was not significantly different from chance using a binomial test with alpha $=$ 0.05. We smoothed the firing rate maps for visualization purposes by binning into a 11 x 16 grid and applying a Gaussian filter with a 1.1 bin standard deviation. Any grid with at least 100 ms spent in it was included in these plots, and all other locations were plotted as white.

Control for epileptic regions

The units from three subjects in our study were localized to what was clinically determined to be the seizure onset zone. To control for a possible confound caused by epileptic activity, we re-calculated the proportions excluding the 15 units from these patients (Patients 2, 10, 12). Our main findings remained consistent after this exclusion: $23/116 = 20\%$ of the units were classified as memory-target cells, $6/116 = 5\%$ as place-like cells, $14/116 = 12\%$ as heading-direction cells, and $9/116 = 8\%$ as memory-related cells.

Acknowledgements

We are grateful to the patients for participating in our study. We thank Shachar Maidenbaum for providing helpful feedback on the manuscript. This work was supported by NIH Grants R01-MH061975, R01-MH104606, S10-OD018211, T32-NS064928 and the National Science Foundation.

References

T. I. Brown, V. A. Carr, K. F. LaRocque, S. E. Favila, A. M. Gordon, B. Bowles, J. N. Bailenson, and A. D. Wagner. *Science*, 352(6291):1323–1326, 2016.

E. F. Chua, D. L. Schacter, E. Rand-Giovannetti, and R. A. Sperling. *Hippocampus*, 17(11):1071–1080, 2007.

T. Danjo, T. Toyoizumi, and S. Fujisawa. *Science*, 359(6372):213–218, 2018.

A. D. Ekstrom. *Hippocampus*, 25(6):731–735, 2015.

A. D. Ekstrom, M. J. Kahana, J. B. Caplan, T. A. Fields, E. A. Isham, E. L. Newman, and I. Fried. *Nature*, 425:184–187, 2003.

R. A. Epstein, E. Z. Patai, J. B. Julian, and H. J. Spiers. *Nature neuroscience*, 20(11):1504, 2017.

I. Fried, C. Wilson, N. Maidment, J. J. Engel, E. Behnke, T. Fields, K. MacDonald, J. Morrow, and L. Ackerson. *Journal of Neurosurgery*, 91:697–705, 1999.

J. L. Gauthier and D. W. Tank. *Neuron*, 99(1):179–193.e7, Jul 2018. doi: 10.1016/j.neuron.2018.06.008.

J. A. Greenberg, J. F. Burke, R. Haque, M. J. Kahana, and K. A. Zaghloul. *NeuroImage*, 114:257–263, Jul 2015. ISSN 1095-9572 (Electronic); 1053-8119 (Linking). doi: 10.1016/j.neuroimage.2015.03.077.

R. A. Gulli, L. Duong, B. W. Corrigan, G. Doucet, S. Williams, S. Fusi, and J. C. Martinez-Trujillo. *bioRxiv*, page 295774, 2018.

P.-Y. Jacob, G. Casali, L. Spieser, H. Page, D. Overington, and K. Jeffery. *Nature neuroscience*, 20(2):173, 2017.

J. Jacobs, M. J. Kahana, A. D. Ekstrom, M. V. Mollison, and I. Fried. *Proceedings of the National Academy of Sciences*, 107(14):6487–6482, 2010.

J. Jacobs, C. T. Weidemann, J. F. Miller, A. Solway, J. F. Burke, X. Wei, N. Suthana, M. R. Sperling, A. D. Sharan, I. Fried, and M. J. Kahana. *Nature Neuroscience*, 16(9):1188–1190, 2013. doi: 10.1038/nn.3466.

S. A. Lee, J. F. Miller, A. J. Watrous, M. Sperling, A. Sharan, G. A. Worrell, B. M. Berry, B. C. Jobst, K. A. Davis, R. E. Gross, B. Lega, S. Sheth, S. R. Das, J. M. Stein, G. Richard, D. S. Rizzuto, and J. Jacobs. *Journal of Neuroscience*, page 218040, 2018.

T. K. Leonard and K. L. Hoffman. *Current Biology*, 27(2):257–262, 2017.

S. Leutgeb, K. Ragozzino, and S. Mizumori. *Neuroscience*, 100(1):11–19, 2000.

J. F. Miller, M. Neufang, A. Solway, A. Brandt, M. Trippel, I. Mader, S. Hefft, M. Merkow, S. M. Polyn, J. Jacobs, M. J. Kahana, and A. Schulze-Bonhage. *Science*, 342(6162):1111–1114, 2013. doi: 10.1126/science.1244056.

J. F. Miller, I. Fried, N. Suthana, and J. Jacobs. *Current Biology*, 2015.

J. F. Miller, A. J. Watrous, M. Tsitsiklis, S. A. Lee, S. A. Sheth, C. A. Schevon, E. H. Smith, M. R. Sperling, A. Sharan, A. A. Asadi-Pooya, G. A. Worrell, S. Meisenhelter, C. Inman, K. A. Davis, B. Lega, P. A. Wanda, S. R. Das, J. M. Stein, R. Gorniak, and J. Jacobs. *Nature communications*, 9(1):2423, 2018.

A. Misra, J. Burke, A. Ramayya, J. Jacobs, M. Sperling, K. Moxon, M. Kahana, J. Evans, and A. Sharan. *Journal of neural engineering*, 11(2):026013, 2014.

R. Morris, P. Garrud, J. a. Rawlins, and J. O'Keefe. *Nature*, 297(5868):681, 1982.

R. Muller. *Neuron*, 17:813–822, 1996.

J. Niediek, J. Boström, C. E. Elger, and F. Mormann. *PLoS One*, 11(12):e0166598, 2016. doi: 10.1371/journal.pone.0166598.

J. O'Keefe and J. Dostrovsky. *Brain Research*, 34:171–175, 1971.

D. B. Omer, S. R. Maimon, L. Las, and N. Ulanovsky. *Science*, 359(6372):218–224, 2018.

S. Qasim, J. Miller, C. Inman, R. Gross, J. Willie, B. Lega, J. Lin, A. Sharan, C. Wu, M. Sperling, et al. *bioRxiv*, 2018.

R. Robertson, E. Rolls, P. Georges-François, and S. Panzeri. *Hippocampus*, 9:206–219, 1999.

E. Rolls and S. O'Mara. *Hippocampus*, 5(5):409–424, 1995.

U. Rutishauser, I. Ross, A. Mamelak, and E. Schuman. *Nature*, 464(7290):903–907, 2010.

F. Sargolini, M. Fyhn, T. Hafting, B. McNaughton, M. Witter, M. Moser, and E. Moser. *Science*, 312(5774):758–762, 2006.

D. L. Schacter and A. D. Wagner. *Hippocampus*, 9:7–24, 1999.

D. Schiller, H. Eichenbaum, E. A. Buffalo, L. Davachi, D. J. Foster, S. Leutgeb, and C. Ranganath. *Journal of Neuroscience*, 35(41):13904–13911, 2015.

W. B. Scoville and B. Milner. *Journal of Neurology, Neurosurgreery, and Psychiatry*, 20:11–21, 1957.

H. Spiers and E. Maguire. *Neuroscience*, 149(1):7–27, 2007.

N. Suthana, A. D. Ekstrom, S. Moshirvaziri, B. J. Knowlton, and S. Y. Bookheimer. *Journal of Neuroscience*, 2009.

J. Taube. *Progress in Neurobiology*, 55(3):225–56, 1998.

J. Taube, R. Muller, and J. Ranck. *Journal of Neuroscience*, 10(2):420–435, 1990.

A. B. Valdez, E. N. Hickman, D. M. Treiman, K. A. Smith, and P. N. Steinmetz. *J Neural Eng*, 10 (1):016001, Feb 2013. doi: 10.1088/1741-2560/10/1/016001.

L. K. Vass, M. S. Copara, M. Seyal, K. Shahlaie, S. T. Farias, P. Y. Shen, and A. D. Ekstrom. *Neuron*, 89(6):1180–1186, 2016.

A. J. Watrous, J. Miller, S. E. Qasim, I. Fried, and J. Jacobs. *eLife*, 7:e32554, 2018.

357 N. Wilming, P. König, S. König, and E. A. Buffalo. *eLife*, 7:e31745, 2018.

358 S. Wirth, P. Baraduc, A. Planté, S. Pinède, and J.-R. Duhamel. *PLoS biology*, 15(2):e2001045, 2017.

359 J. T. Wixted, L. R. Squire, Y. Jang, M. H. Papesh, S. D. Goldinger, J. R. Kuhn, K. Smith, D. Treiman,
360 and P. N. Steinmetz. *Proceedings of the National Academy of Sciences*, 111(26):9621–9626, 2014.

Patient number	Age	Gender	# Sessions	Task version	# MTL Behnke-Fried bundles	# MTL units	Electrode locations
1	22.7	M	1	object cued	2	4	R SUB, R HPC
2	52.3	M	2	object cued	6	3	L AMY, L HPC, R EC, R SUB, R HPC
3	41	M	1	object cued	1	2	L HPC
4	22.4	M	3	object cued	1	5	R EC
5	21.5	F	2	object cued	2	7	L HPC, L SUB
6	25.6	F	1	object cued	2	11	R EC
7	29.4	M	2	object cued	2	9	L SUB, L PRC
8	23.4	F	1	object cued	1	1	R HPC
9	21.9	F	3	object cued	2	39	L EC
10	27.6	M	1	object cued	2	4	L SUB, L PHC
11	47	M	1	object cued	1	8	L EC
12	20	M	1	object cued	1	8	R EC
13	21	M	1	location cued	2	12	L HPC, R HPC
14	55	M	1	location cued	2	2	R HPC, R PHC
15	43.5	F	2	location cued	2	16	L HPC, R SUB

Table 1: Patients and unit information. *Table indicates each patient's demographics and their MTL unit counts. R/L: right/left; HPC: hippocampus, SUB: subiculum, AMY: amygdala, EC: entorhinal cortex, PRC: perirhinal cortex, PHC: parahippocampal cortex.*